

A Glance at the Standard Map

by Ryan Tobin

Abstract

The Standard (Chirikov) Map is studied and various aspects of its intricate dynamics are discussed. Also, a brief discussion of the famous KAM theory that describes the dismemberment of invariant tori and the onset of chaos. Stable/unstable manifolds from a fixed point is portrayed.

Introduction

Two-dimensional area-preserving map functions have produced many important insights into nonintegrable Hamiltonian systems that would be too complicated to study otherwise. These maps approximate a Poincaré section for Hamiltonian systems. The interesting dynamics of these 2-D maps provide theoretical framework that can be applied to many areas of physics. One pioneer in this work, Boris Chirikov, contributed much progress to the understanding of chaos in Hamiltonian systems. He also developed the Standard (Taylor-Chirikov) area-preserving map defined as (in this paper):

$$\begin{aligned}\theta_{n+1} &= \theta_n + p_{n+1} \equiv f, & \text{modulo } 1 \\ p_{n+1} &= p_n + K/(2\pi) \sin(2\pi\theta_n) \equiv g, & \text{modulo } 1\end{aligned}\tag{1}$$

In this way the mappings always reside on the unit square. This map was first discovered by Bray Taylor and then was later proposed by Boris Chirkov to model magnetic field lines. θ and p can be considered to respectively represent the position and momentum of a pendulum with an impulsive torque $K\sin(x)$ at the end of the pendulum. K represents the amplitude of the “kicks” and determines the extent of nonlinearity of the system.

The mapping (1) exhibits various properties, at least locally, of many different systems. The measure of nonlinearity, K , influences the amount of chaos in the dynamics. This map is an example of an area-preserving map because the area of the phase space never shrinks or expands as is shown by computing the determinant of the Jacobian.

$$\det J = \begin{vmatrix} \frac{\partial f}{\partial \theta_n} & \frac{\partial f}{\partial p_n} \\ \frac{\partial g}{\partial \theta_n} & \frac{\partial g}{\partial p_n} \end{vmatrix} = \begin{vmatrix} (1 + K\cos(2\pi\theta_n)) & 1 \\ K\cos(2\pi\theta_n) & 1 \end{vmatrix} = 1.\tag{2}$$

Since, it is equal to one there is no shrinking or stretching.

Periodic/Quasiperiodic Orbits

Consider the case when $K = 0$. (1) reduces to

$$\begin{aligned} p_{n+1} &= p_n, \text{ (mod } 1) \\ \theta_{n+1} &= \theta_n + p_{n+1}, \text{ (mod } 1) \end{aligned} \quad (3)$$

which is integrable and has the obvious solution $\theta_n = \theta_0 + np_0 \text{ (mod } 1)$ and $p_n = p_0 \text{ (mod } 1)$. Every orbit lies on an invariant torus. The orbits can exhibit periodic or quasiperiodic behavior depending on the initial conditions. If $p_0 = M/N$ for some M, N integers, then trajectory is a period- N orbit. Otherwise, for irrational p_0 the orbit is quasiperiodic and densely fill in the torus.

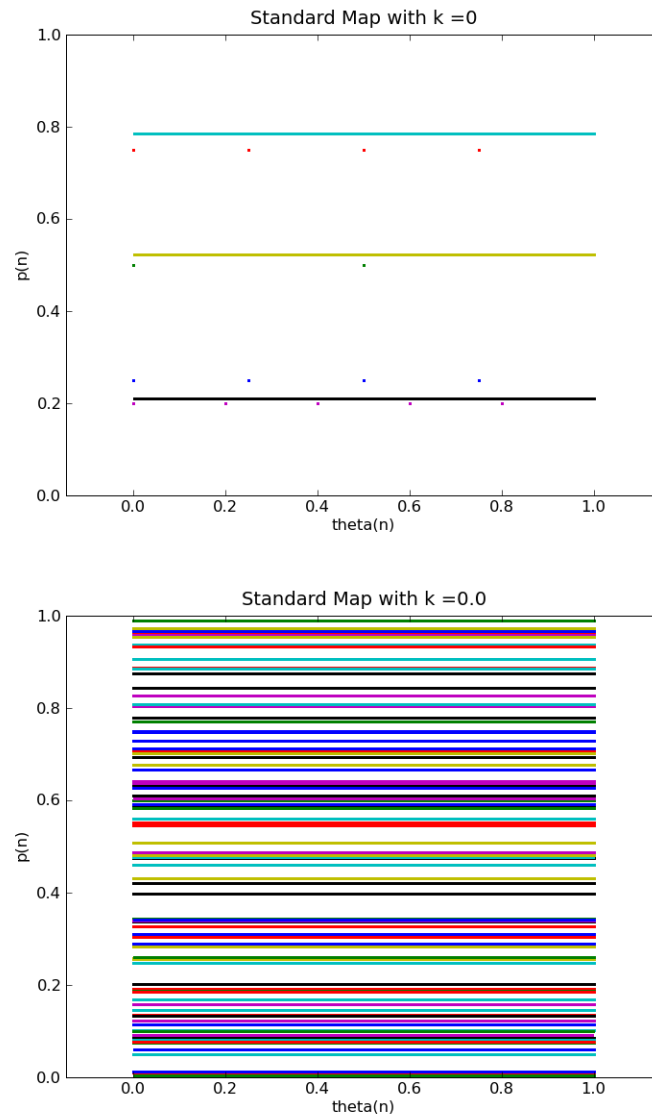


Figure 1: (TOP) A plot of several trajectories for the case with no nonlinear dependence. The trajectories start with $p_0 = \pi/4, 3/4, \pi/6, 1/2, 1/4, \pi/15, 1/5$. Notice the fixed period-N orbits. (BOTTOM) A plot of many quasiperiodic orbits

If K is slightly perturbed from 0, we can see that the basic structure is maintained. It seems that the orbits still traverse horizontally and densely fill the torus. For small K , (1) can be approximated well by derivative, and thus the dynamics are still integrable and most of the invariant tori remain for sufficiently small K .

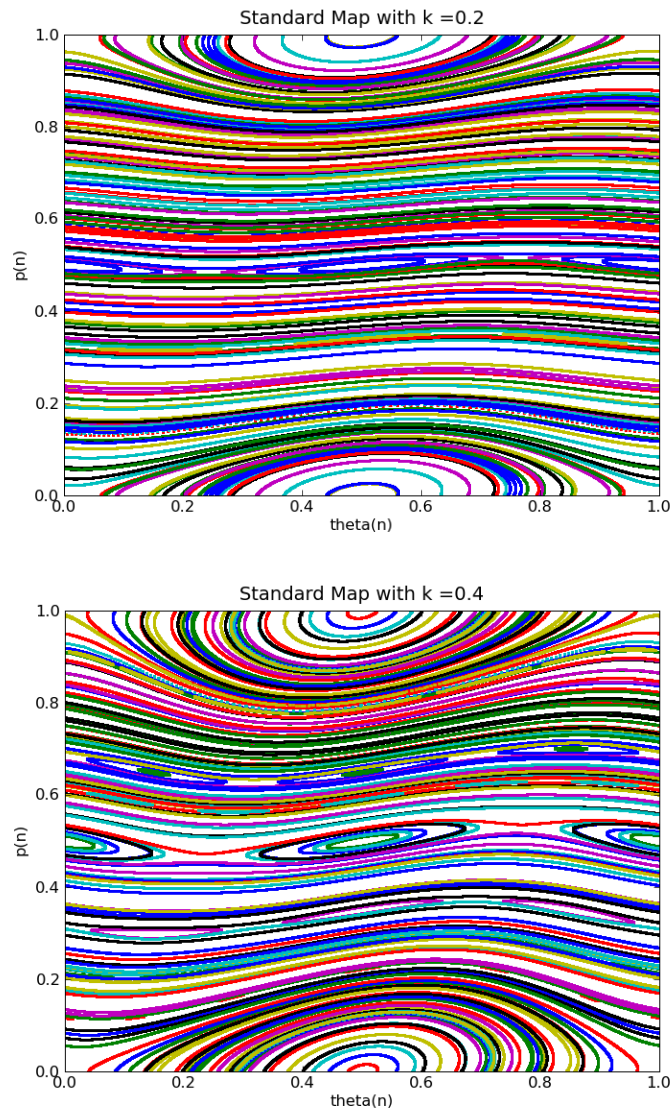


Figure 2: A plot of many trajectories for $K=0.2$ and $K=0.4$. Notice the nonlinear resonances begin to form and grow with K .

Nonlinear Resonance

We notice that not all of the orbits are part of invariant tori. In fact, we actually have some ellipses encircling the period-1 fixed point at $(0.5, 0)$. I will refer to such circles as “islands”. These circles don’t rotate the torus and are bounded by a separatrix curve that segregates the different types of orbits.

We can see that Figure 2 closely resembles the phase space of a pendulum. For small K the size of the island increases with K . Also, for increasing K , the island seems to disfigure into an almost increasingly sinusoidal stretching, if it can be called that.

Fixed Points and Linearization

The fixed points of the pendulum lie at antipodal ends corresponding to $\theta=0,.5$ and $p=0$. We see that this also appears true in figure 2.

$$\begin{aligned}\theta &= \theta + p \quad , (mod\ 1) \\ p &= p + K/2\pi \sin(2\pi\theta) \quad , (mod\ 1)\end{aligned}\tag{4}$$

The fixed points are $\theta=0,.5$ and $p=0$. Directly analogous to the simple pendulum. Since $\det(J) = 1$, the eigenvalues, and thus the stability, of the fixed points are completely determined by $Tr(J)$.

$$Tr(J) = 2 + K\cos(2\pi\theta) .\tag{5}$$

We can classify the stability of the fixed points based on the eigenvalues and corresponding eigenvectors of the linearized Jacobian (Strogatz). So,

$$\begin{aligned}\lambda_{1,2} &= \frac{1}{2} \left[Tr(J) \pm \sqrt{Tr(J)^2 - 4\Delta} \right] = \frac{1}{2} \left[2 + K\cos(2\pi\theta) \pm \sqrt{K^2\cos^2(2\pi\theta) + 4K\cos(2\pi\theta)} \right] \\ v_{1,2} &= \left(\frac{1}{-\frac{K}{2}\cos(2\pi\theta) \pm \frac{1}{2}\sqrt{K^2\cos^2(2\pi\theta) + 4K\cos(2\pi\theta)}} \right)\end{aligned}\tag{6}$$

and $|Tr(J)| < 2$ implies fixed point is a center, while $|Tr(J)| > 2$ implies fixed point is a saddle point.

We find that (0,0) is unstable for $K > 0$ and (.5,0) stable for $0 < K < 4$. These remarks are somewhat apparent in Figure 2.

Twist Dynamics

One way to get a feel for the way the maps dynamics behave is by looking at its twist features. It can be noticed that the displacement between successive θ increases with increasing p . This is better understood by plotting a line segment of initial conditions for only several iterations. Figure 3 shows how successive iterations tend to twist about the fixed points.

Manifolds

For each period-N orbit, there are corresponding stable and unstable directions that protrude from the fixed point. For example, a saddle point is evidently at the origin. From stable/unstable manifold theory, we can conjecture that there are manifolds that protrude

from these fixed points and trajectory that has an initial value on the manifold will remain on the manifold indefinitely. The unstable and stable sets, W^U and W^S , of an invariant set are defined as

$$\begin{aligned} W_A^S &\equiv \{(x, y): f^n(x, y) \rightarrow \lambda \text{ as } n \rightarrow \infty\} \\ W_A^U &\equiv \{(x, y): f^n(x, y) \rightarrow \lambda \text{ as } n \rightarrow -\infty\} \end{aligned} \quad (7)$$

Where n represents the n th iterate of the standard mapping function f .

When Λ represents a saddle point, the eigenvectors point in the directions of the submanifolds.

I tried numerous techniques to plot the manifolds and all ended up erroneous. Then I noticed that when I iterated a line segment it would warp until the point where it would start to trace out squiggly lines around the $(.5, 0)$ fixed point (figure 4). I tried more iterations and found an iteration that seemed to map out what looked like to me trace out the unstable manifold in the vicinity of the fixed point (figure 5). We can tell it's the unstable manifold because of the eigenvectors.

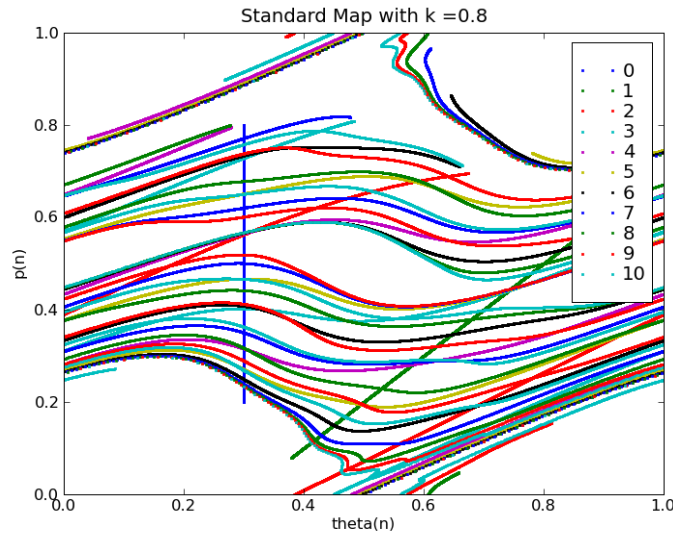


Figure 3: Iteration of an initial line segment. Notice squiggly lines near $(.5, 0)$. Also note that this map is shifted to place the fixed point in the middle of the screen. So this point $(.5, 0)$, corresponds to the $(0, 0)$ point in previous plots.

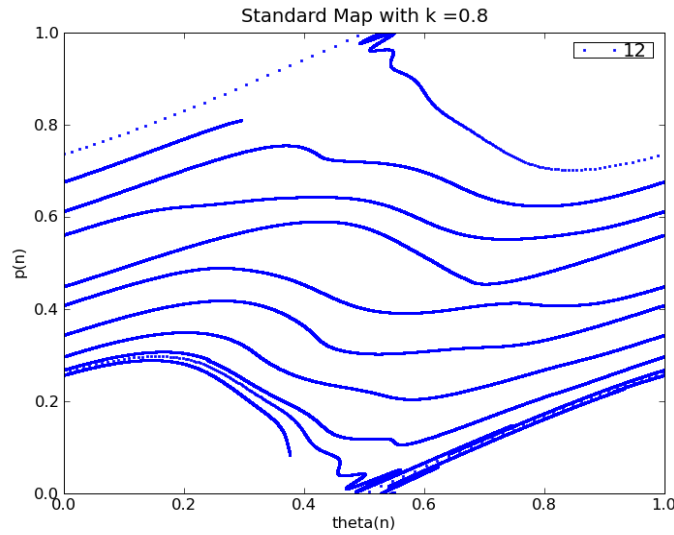


Figure 4: After the same initial conditions iterated 12 times, we can begin to see what looks like the outlines of the unstable manifold.

I changed (1) so as to view the period one fixed point in the center of the plot:

$$\begin{aligned} \theta_{n+1} &= \theta_n + p_{n+1} \equiv f, & \text{modulo } 1 \\ p_{n+1} &= p_n + K/(2\pi) \sin(2\pi\theta_n) \equiv g, & \text{modulo } 1 \end{aligned} \quad (8)$$

I tried a very small (of order $1e-4$ in length), dense, initial line segment along the unstable eigen-direction of the period-1 fixed point. The line segment stretched along the heteroclinic orbit and seemed to come around and squiggle along the other eigen-direction (figure 5). It would be interesting to study interaction of the opposing manifolds and it has been done in great detail (Meiss 1992), but I ran out of time to do so.

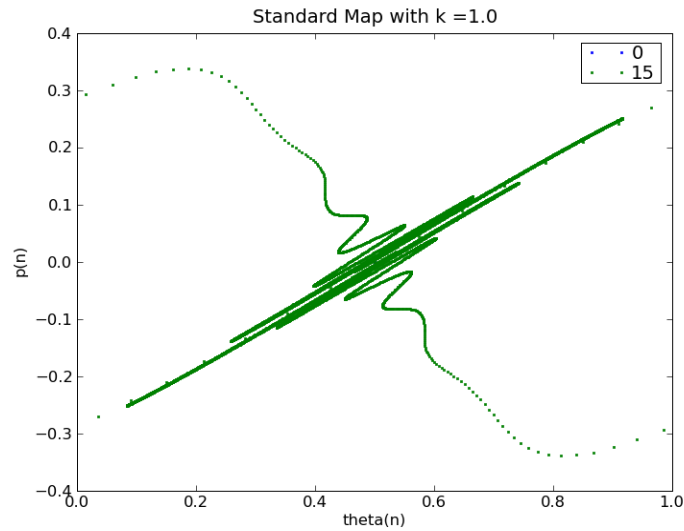


Figure 5: Plot of manifold from iteration of small line segment with slightly larger K .

Destruction of Invariant Tori

As K increases, the nonlinearity of the system increases. The size of the islands will likewise increase. We can see the region where the invariant tori live, is slowly swallowed up with increasing K . Since an invariant torus exist between two resonances, eventually an heteroclinic trajectory will break through the invariant torus joining the two resonances via their opposing manifolds. But this implies that the invariant torus must break because trajectories cannot overlap in 2D.

It was Chirikov who initiated investigations into when this occurred. He created a way to approximate when this happened, which was later improved upon. KAM Theory delves into the study of the moments when the invariant tori are dismembered.

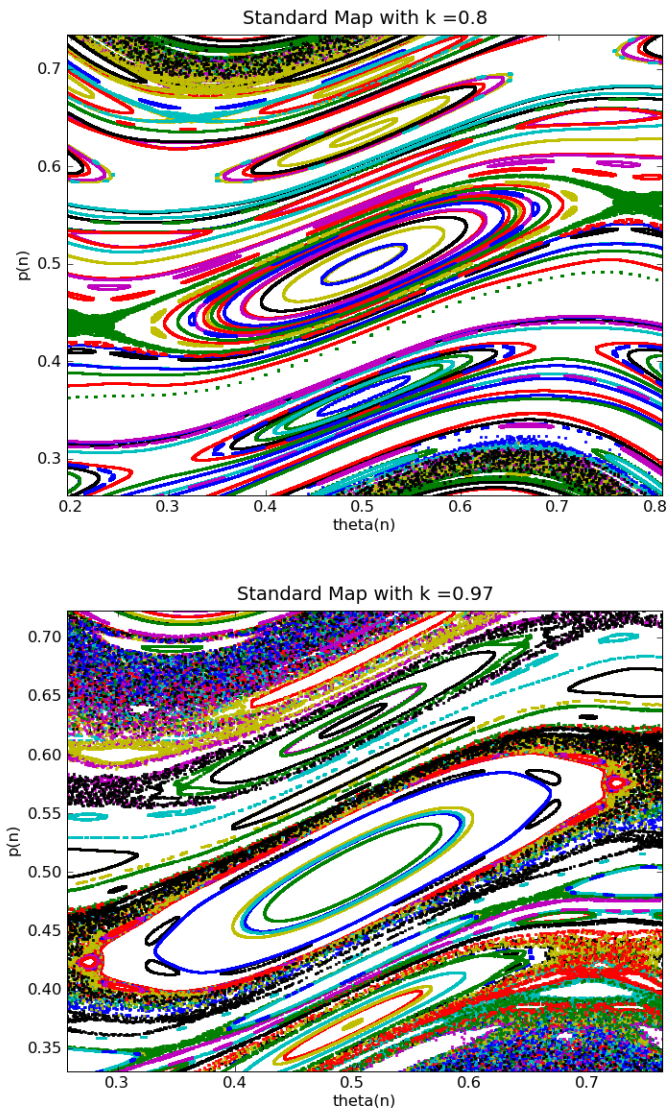


Figure 6: We can see that much of the invariant tori in the top image have been destroyed in the bottom. In fact, there are almost no invariant tori left in the bottom figure.

KAM Theory

The Kolmogorov-Arnold-Moser theorem declares that if the Hamiltonian of a system is nonintegrable, then the only orbits that are not destroyed are orbits with irrational winding numbers that are quasiperiodic. In the 2-D mapping of the Poincaré plane, these trajectories show up as continuous orbits around fixed points. The quasiperiodicity of the trajectories tells that the mapping will never land on the same point the 2D Poincaré plane. This results in a smooth curve (if sufficient quantities of iterations are computed). These orbits are called invariant (KAM) tori.

Kam theory predicts that frequencies that are sufficiently irrational correspond to the longest living invariant tori.

As the nonlinearity factor, K , is increased, the nonintegrable components of the map become more apparent. The final invariant torus is destroyed at the point where the irrationality of the winding number corresponding to the last quasiperiodic orbit is “farthest” from rational. This occurs at the golden-mean ($\frac{1}{2} + \frac{\sqrt{5}}{2} \approx 1.61$).

Fractal Structure and Chaos

Upon zooming in on the edges of some of these nonlinear resonances, we see that there are even smaller islands that mimic the behavior of the larger ones. In fact all this talk of manifolds and invariant tori, can also be seen on this smaller scales as well. There are infinite many fixed points due to the fact that there are infinite many rational numbers corresponding to some period- n orbits.

We can see this in this in the different plots of figure 7.

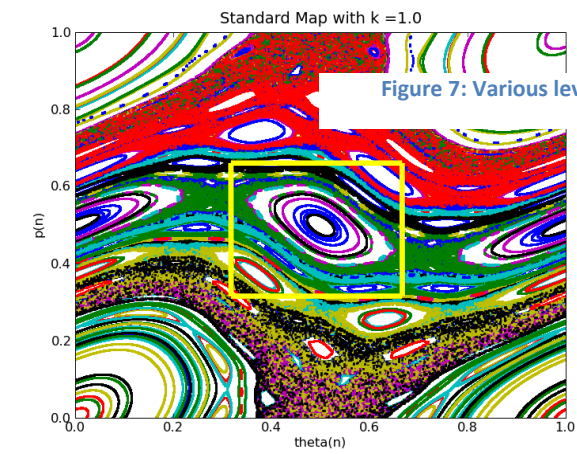
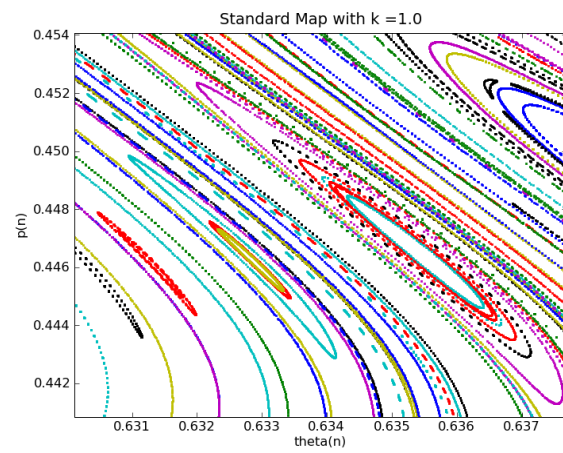
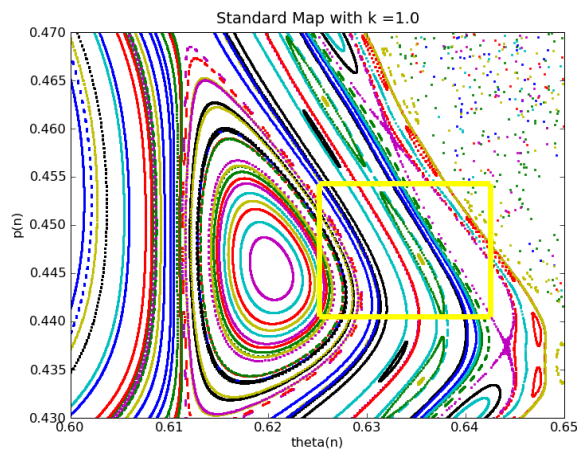
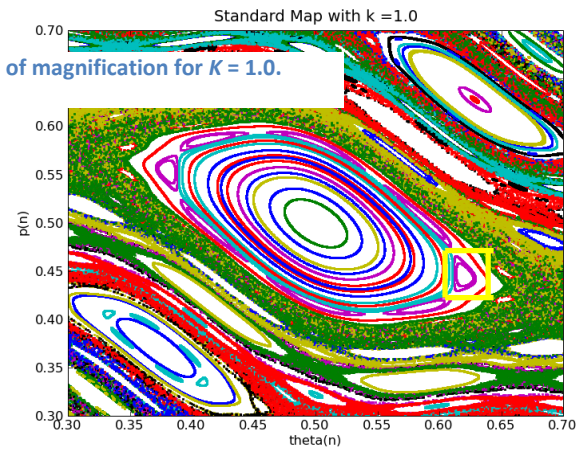


Figure 7: Various levels of magnification for $K = 1.0$.



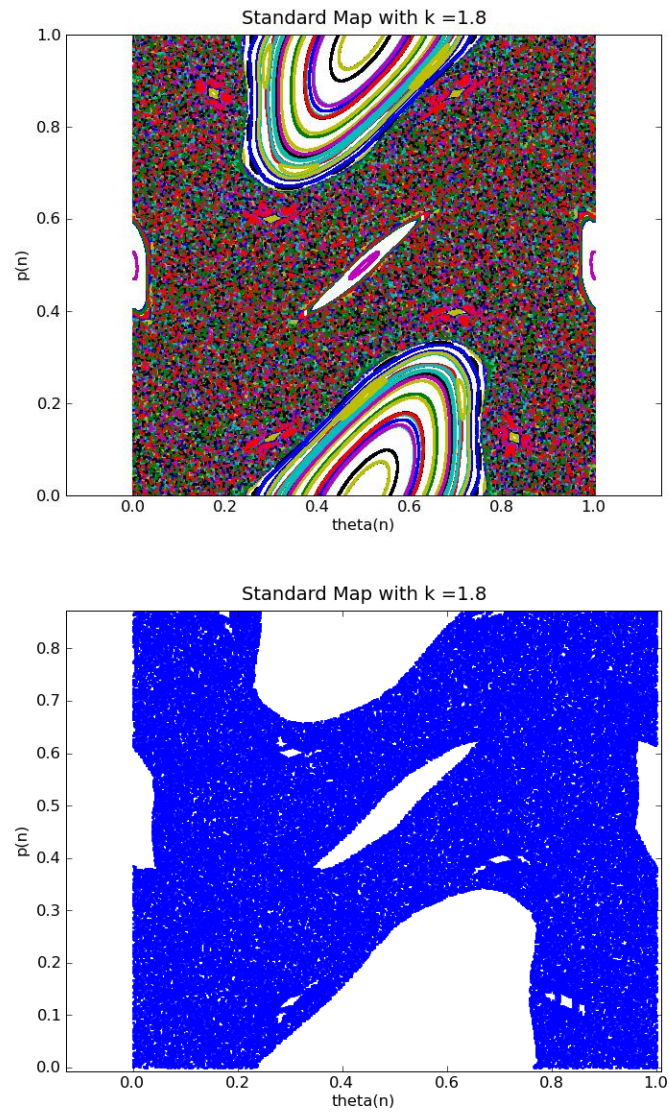


Figure 8: (TOP) After global chaos has occurred. (BOTTOM) A single trajectory demonstrating that chaos has taken over.

References

Chirikov B.V., "Research concerning the theory of nonlinear resonance and stochasticity",
Preprint N 267, Institute of Nuclear Physics, Novosibirsk (1969), (Engl. Trans., CERN
Trans. 71-40 (1971))

Meiss, J. D. , "Symplectic Maps, Variational Principles, and Transport" 1992 APS

Strogatz, S. *Nonlinear Dynamics and Chaos*. Reading, MA: Addison-Wesley, 1994